Influence of minimally invasive endodontic access cavities and bonding status of resin composites on the mechanical property of endodontically-treated teeth: A finite element study

Fei Lin[a,], Ronald Ordinola-Zapata[b], Alex S.L. Fok[c], Roy Lee[b]*

[a] *Department of Cariology and Endodontology, Peking University School and Hospital of Stomatology, Beijing 100081, China*
[b] *Division of Endodontics, Department of Restorative Sciences, School of Dentistry, University of Minnesota, Minneapolis, MN 55455, USA*
[c] *Minnesota Dental Research Center for Biomaterials and Biomechanics, School of Dentistry, University of Minnesota, Minneapolis, MN 55455, USA*

ARTICLE INFO

ABSTRACT

Objective: To study the mechanical behavior of endodontically-treated teeth with minimally invasive endodontic access cavities and resin composite restorations under different bonding conditions using finite element analysis (FEA).

Methods: Four Class-II endodontic access cavities including the mesio-occlusal minimally-invasive (MO-MIE), mesio-occlusal conventional (MO-CONV), disto-occlusal minimally-invasive (DO-MIE), and disto-occlusal conventional (DO-CONV) cavities were prepared in 3D-printed maxillary first molars. Each tooth was subjected to root canal preparation and scanned using micro-CT to provide a 3D structural model which was virtually restored with resin composite. An intact 3D-printed molar was used as control. FEA was conducted under a 250-N vertical load. Three different interfacial bonding conditions between dentin/enamel and resin composite were considered, i.e. fully bonded, partially debonded, and fully debonded. The maximum principal stress of dentin and the normal tensile stress at the interfaces were recorded. The risk factor of failure for each component was then calculated.

Results: In the fully-bonded tooth, the dentin-composite interface showed significantly higher stress and a higher risk factor than dentin, indicating that debonding at the dentin-composite interface would occur prior to dentin fracture. With the dentin-composite interface debonded, the enamel-composite interface exhibited higher stress and a higher risk factor than dentin, indicating that debonding at the enamel-composite interface would occur next, also prior to dentin fracture. With the resin composite fully debonded from the tooth, stress in dentin increased significantly. Irrespective of the bonding status, the CONV groups exhibited higher median stresses in dentin than the MIE groups.

Significance: Within the limitation of this study, it was shown that debonding of the resin composite restoration increased the stress in dentin and hence the risk of dentin fracture in endodontically-restored teeth. Minimally-invasive access cavities could better safeguard the fracture resistance of interproximally-restored teeth compared to conventional ones.

1. Introduction

Caries is one of the most common etiologies of pulpal diseases [1]. To eliminate bacteria and inflamed tissues from the root canal system, an access cavity is required to provide access for endodontic instruments and irrigants. When caries is extensive and involves the proximal marginal ridges, a Class-II cavity is required together with the access cavity [2,3]. The loss of tooth structure has proved to make a tooth less resistant to fracture under high occlusal forces [4,5]. Hence, there is a common consensus that the extent of dentin removal should be minimized to achieve the goals of endodontic treatment [6,7].

Conventional endodontic access cavities require removing the entire pulp chamber roof and establishing straight-line access to the canal orifices [8,9]. However, with the adoption of magnification and the development of heat-treated NiTi instruments, the root canal system can be mechanically treated with smaller access cavities [10,11]. Though controversial, it has been reported that using smaller access cavities would not compromise the efficacy of infection control of the root canal system [10,12].

Another clinical problem with endodontically-treated teeth is the failure of resin composite restorations, more specifically, debonding [13]. This may lead to coronal leakage, marginal discoloration and secondary caries [14,15]. Debonding could be caused by polymerization shrinkage of the resin composite, aging and degradation of the restorative materials, contamination of the gingival walls, among others, especially in Class-II restorations [2,3,16,17]. The effect of debonding of the resin composite restoration on the fracture resistance of endodontically-treated teeth has seldom been considered, especially those with minimally invasive access cavities [18–23].

As a computational technique for evaluating stress distributions, finite element analysis (FEA) has been widely used in dentistry modeling the mechanical behavior of dental restorations of different materials or structural designs [2,3]. It allows one to focus on the effect of a particular factor in the absence of confounding issues that may occur during in vivo or in vitro studies [24]. Moreover, with the help of 3D imaging techniques such as micro-computed tomography (micro-CT), the mechanical behavior of complex tooth structures could be analyzed with anatomically accurate models [25,26]. Thus, the effect of both cavity designs and bonding conditions of the resin composite could be fully simulated through FEA, which would help us better understand the mechanical behavior and failure of endodontically-treated teeth.

Hence, this study aimed to investigate the influence of endodontic access cavity design on the mechanical behavior of endodontically-treated teeth, comparing conventional and minimally-invasive access cavities, using FEA. The bonding condition of the dentin-composite and enamel-composite interfaces and the involvement of the marginal ridge (mesial or distal) were also considered.

2. Materials and methods

2.1. Designs of access cavities

Four different designs of access cavities were prepared in identical 3D-printed maxillary first molars (#3–01, Dental Engineering Laboratories, Santa Barbara, CA, USA) by an experienced endodontist as follows (Fig. 1a):

– MO-MIE: a Class-II mesio-occlusal restorative cavity with a minimally-invasive endodontic access cavity,
– MO-CONV: a Class-II mesio-occlusal restorative cavity with a conventional endodontic access cavity,
– DO-MIE: a Class-II disto-occlusal restorative cavity with a minimally-invasive endodontic access cavity, and
– DO-CONV: a Class-II disto-occlusal restorative cavity with a conventional endodontic access cavity.

The conventional access cavity followed the classical principles of a straight-line access and complete removal of the pulp chamber roof. For the minimally-invasive access cavity, an opening was created until all the canal orifices could be seen under the microscope, no additional tooth structure was removed to provide a straight-line access. The pulp chamber was partially unroofed. The root canals were then sequentially prepared to apical sizes of #30.04 in the buccal canals, #25.04 in the mesiolingual canal and #40.04 in the palatal canal using Vortex Blue instruments (Dentsply Tulsa Dental, Tulsa, OK, USA). All the procedures were performed under approximately 8X magnification (Global, USA). An intact 3D-printed molar was used as control.

2.2. Finite element models

The prepared 3D-printed teeth were scanned using a micro-CT scanner (HMX-XT 225, Nikon Metrology Inc., Brighton, MI, USA) with a 0.5-mm thick aluminum filter. The following scanning parameters were used: 20-μm isotropic resolution, 115-kV accelerating voltage, 90-μA beam current, 720 projections, 4 frames/projection, and 708-ms exposure time. 3D spatial reconstruction of the teeth was performed using CT Pro 3D XT 3.1.11 (Nikon Metrology Inc., Brighton, MI, USA) and visualized using VGSTUDIO MAX 3.1 (Volume Graphics GmbH, Heidelberg, Germany). The whole structure was segmented into the different components, i.e. enamel, dentin, the pulp chamber and root canal systems, based on their
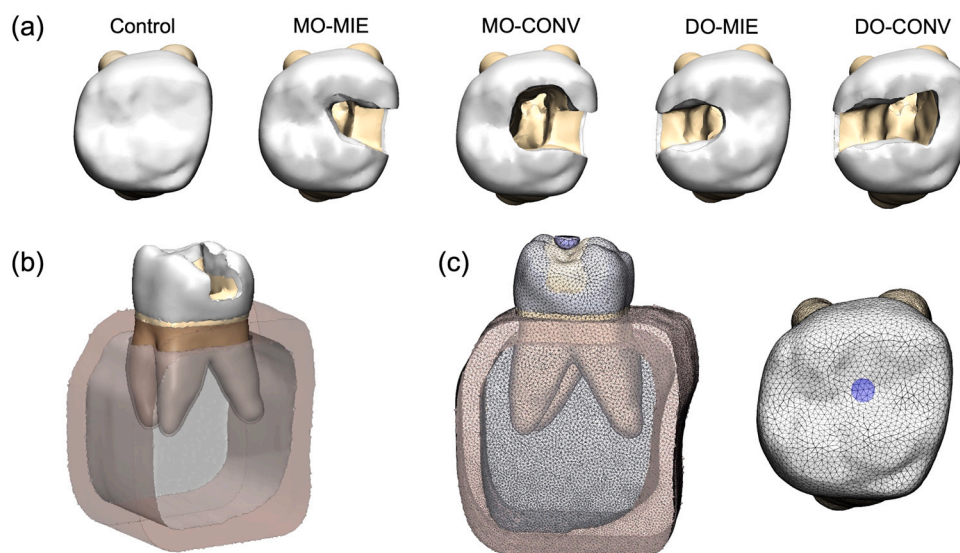
Fig. 1 – (a) Different designs of access cavities. (b) A reconstructed sample model with cortical bone and cancellous bone around the tooth. (c) The 250-N vertical load applied through a hemisphere in the FEA.

different densities or gray values in the images. The thickness of enamel was ~2.5 mm at the cusps and ~0.5 mm at the cementoenamel junction in accordance with human maxillary first molars [27,28]. 3D structural models (Fig. 1b) were subsequently created using the software Mimics Research 19.0 and 3-Matic Research 11.0 (Materialise HQ, Leuven, Belgium). All the cavities were virtually restored with resin composites which were generated by subtracting the models with access cavities from the intact one. Supporting structures including the periodontal ligament, lamina dura, cortical bone and cancellous bone were virtually constructed around the tooth roots based on their actual anatomy (Fig. 1b). The thickness of the cortical bone was 2 mm while the distance between the cortical bone and the cementoenamel junction was ~3 mm, assuming normal periodontal conditions.

2.3. FEA

The Abaqus software (SIMULIA, Dassault Systèmes, Johnston, RI, USA) was used to perform the stress analysis. All the materials were considered homogeneous, linearly elastic and isotropic. The Young's moduli and Poisson's ratios were assigned according to values from the literature (Table 1). Each

model was meshed with isoparametric tetrahedral elements and verified by a convergence test with increasing mesh density. The numbers of elements and nodes were, respectively, 359840 and 82272 for the control, 359046 and 82437 for MO-MIE, 363050 and 84071 for MO-CONV, 371367 and 84583 for DO-MIE, and 360652 and 82932 for DO-CONV. All the regions were assumed to be fully tied to each other to begin with. Three different interfacial bonding conditions between dentin/enamel and the resin composite were then explored:

– Fully bonded: the resin composite was fully bonded to both dentin and enamel.
– Partially debonded: the resin composite was debonded from dentin but not from enamel. The surface-to-surface interaction between dentin and composite was set as frictionless, while enamel and the resin composite remained fully tied to each other.
– Fully debonded: the resin composite was debonded from both dentin and enamel. The surface-to-surface interaction between dentin/enamel and the resin composite was set as frictionless.

A 250-N compressive load was applied vertically by descending a 3-mm-diameter loading sphere onto the central fossa of each tooth model to simulate a typical biting force [29] (Fig. 1c). The frictional coefficient between the sphere and the tooth was set at 0.3. The mesial and distal surfaces of the cortical bone were fully constrained while those of the cancellous bone were constrained in only the mesial-distal direction. The distribution of the maximum principal stress (MPS) was determined for each model. Cuspal flexure of the models in the buccopalatal direction was also plotted. The peak and median MPS values for dentin and the normal tensile stress at the dentin-composite and enamel-composite interfaces were then calculated.

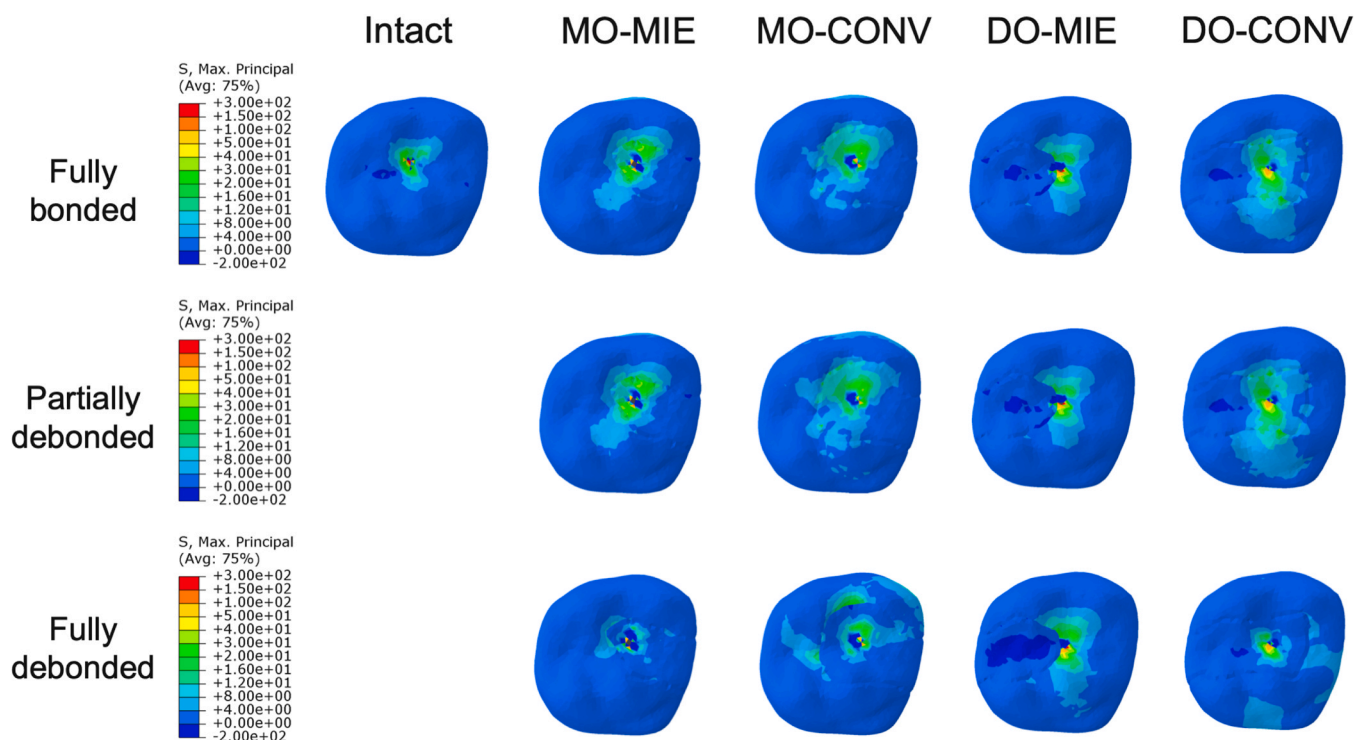| Table 1 – Material properties used in FEA.		
Material	Young's modulus (GPa)	Poisson's ratio
Enamel [39]	84.1	0.3
Dentin [40]	18.6	0.3
Resin composite [41]	12	0.3
Periodontal ligament [42]	0.0689	0.45
Cortical bone [43]	13.7	0.34
Cancellous bone [43]	1.37	0.3

Fig. 2 – Distributions of MPS (MPa) on the occlusal surfaces of different models with different bonding conditions.

2.4. Risk factor calculation

The risk factor of a structure is defined as the ratio of the failure-causing stress in the structure to the strength of the material it is made of [30,31]. It indicates the risk of failure of the structure under a certain load. A risk factor lower than 1 means that the stress is at an allowable level. If the risk factor is greater than 1, the structure is likely to fail. The risk factors of dentin, the dentin-composite interface, and the enamel-composite interface were calculated for each model. Their respective strengths were 114 MPa, 10.6 MPa and 15.6 MPa according to the literature [32–35].

3. Results

3.1. Stress distributions of fully-bonded teeth

In the fully-bonded teeth, the MPS concentrated around the loading point on the occlusal enamel surface (Fig. 2), with the intact tooth having the smallest stress concentration area. The stress concentration areas in the teeth with the CONV design were larger than those in the teeth with the MIE design for both MO and DO cavities. In the DO-CONV tooth, the stress concentration (~5 MPa) extended to the mesial-palatal cusp (Fig. 2). The same region in the teeth with the DO-MIE or MO cavity had lower stresses.

Within the coronal and root dentin, the peak MPS of the DO models was lower than that of the MO models (Fig. 3 and Table 2). The median MPS of the two teeth with the MIE design was slightly lower than that of the CONV teeth.

At the dentin-composite interface, normal tensile stresses of 0.5–8 MPa were found at the buccal and lingual walls of the proximal cavities in all the models (Fig. 4). The peak normal tensile stress at the interface (Table 3) was significantly higher than the peak MPS of dentin (Table 2) in all the models. The teeth with the MO cavity showed higher median interfacial stresses than the median MPS in dentin, while those with the DO cavity showed similar median interfacial stresses as the median MPS in dentin. The teeth with the DO cavity had lower peak and median interfacial stresses than those with the MO cavity (Table 3). The median stresses of the teeth with the MIE design were lower than those with the CONV design.

The risk factors of the dentin-composite interfaces of all the models were much higher than those of dentin (Table 4), indicating that debonding of the dentin-composite interface would occur prior to the fracture of dentin. Among the four models, those with the MO cavity showed higher risk factors at the dentin-composite interface than those with the DO cavity.

3.2. Stress distributions of partially-debonded teeth

With the dentin-composite interface debonded, the peak MPS of all the models was still found around the loading point on the occlusal enamel surface (Fig. 2). Again, there were larger stress concentration areas with the CONV design than with the MIE design. Compared with the fully-bonded teeth, the partially-debonded CONV models showed more extended stress concentration regions towards the palatal side and cervical dentin while the partially-debonded MIE models showed similar stress concentration regions (Fig. 2).
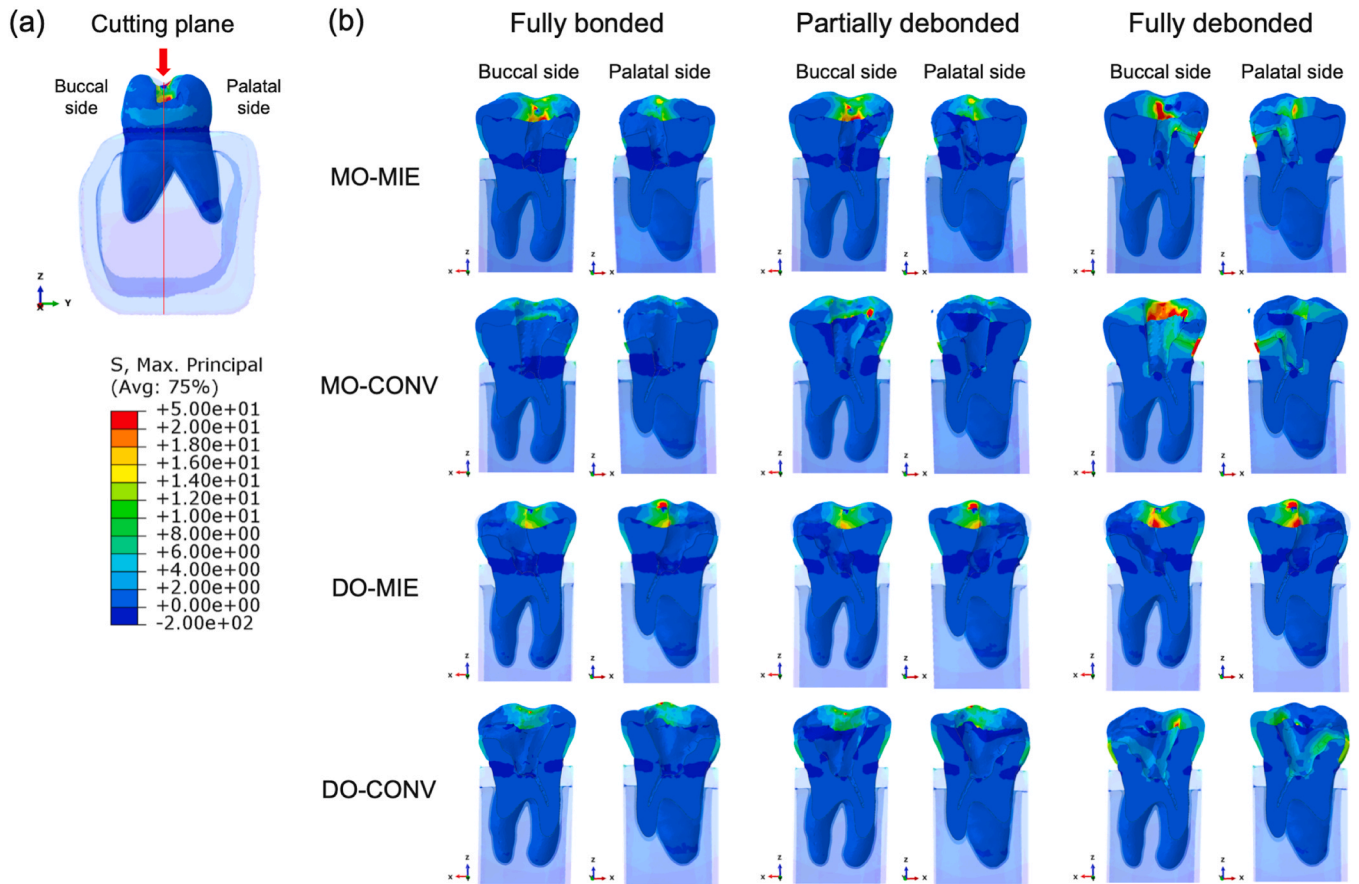
Fig. 3 – (a) Cutting plane of the tooth to reveal dentin stresses. (b) Distributions of MPS (MPa) of different models under different bonding conditions from sectional views.

The peak MPS of coronal dentin increased significantly in all the models (Fig. 3 and Table 2). There was a slight increase in the median MPS of coronal and root dentin (Fig. 5 and Table 2). The CONV models exhibited higher peak and median MPS in both coronal and root dentin than the corresponding MIE models.

Since the resin composite was debonded from dentin, there was zero interfacial normal tensile stress at the dentin-composite interface (Fig. 4). The normal tensile stresses at the enamel-composite interface (Table 3) were significantly higher than the MPS of dentin (Table 2).

The risk factors of the enamel-composite interface were higher than those of dentin, indicating that failure of the enamel-composite interface would occur next, prior to dentin fracture (Table 4).

| Table 2 – Peak and median values of MPS of dentin (MPa).							
			Intact	MO-MIE	MO-CONV	DO-MIE	DO-CONV
Coronal dentin	Fully bonded	Peak	1.98	2.79	2.79	1.8	2.69
		Median	0.19	0.21	0.25	0.2	0.31
	Partially debonded	Peak	–	6.49	39.87	3.44	5.37
		Median	–	0.21	0.3	0.21	0.36
	Fully debonded	Peak	–	20.77	17.32	3.24	10.91
		Median	–	0.32	0.51	0.25	0.8
Root dentin	Fully bonded	Peak	2.11	3.11	2.79	1.8	1.69
		Median	0.09	0.11	0.13	0.09	0.1
	Partially debonded	Peak	–	2.07	3.61	1.92	2.53
		Median	–	0.12	0.17	0.1	0.15
	Fully debonded	Peak	–	5.75	7.31	1.75	6.27
		Median	–	0.18	0.21	0.1	0.21
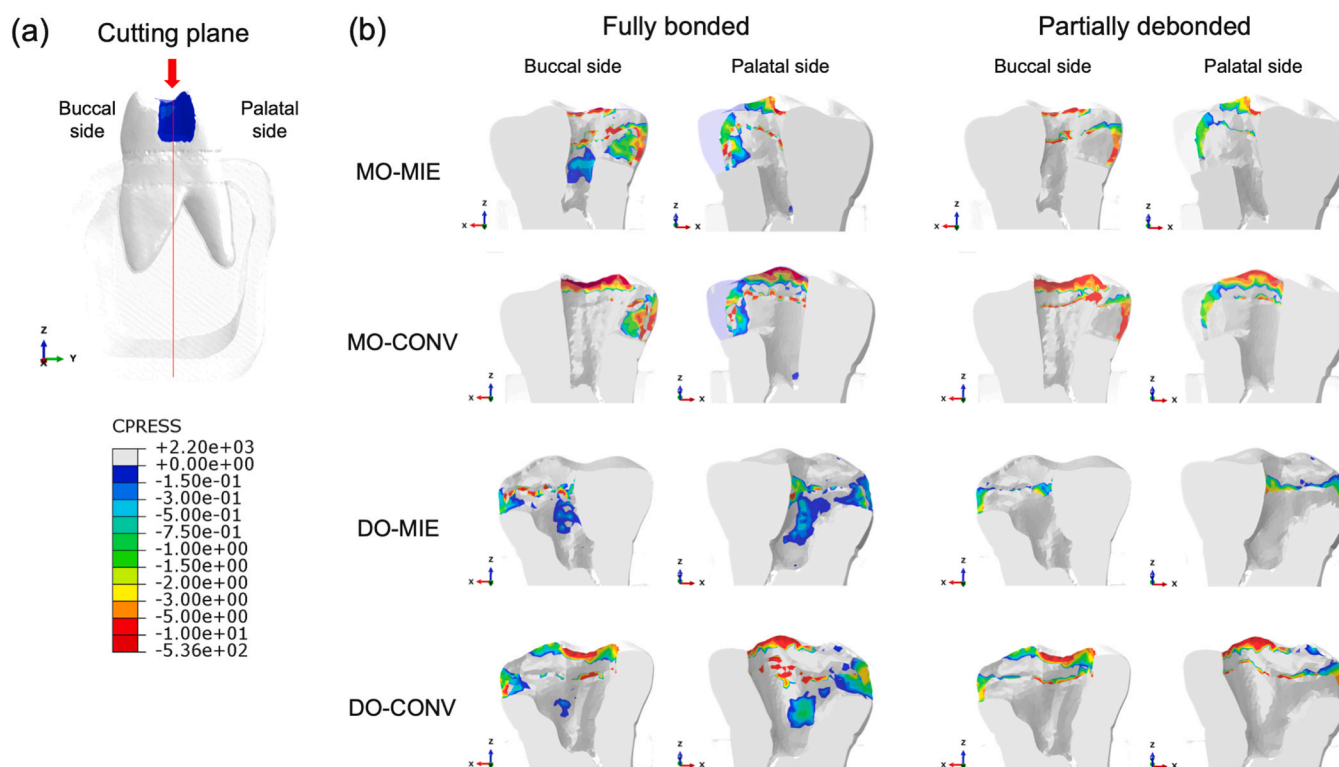
Fig. 4 – (a) Cutting plane of tooth to reveal interfacial stresses. (b) Distributions of interfacial normal stress (MPa) from buccal and palatal sides of the fully-bonded and partially-debonded teeth.

Table 3 – Peak and median values of the normal tensile stress at the interfaces (MPa).						
			MO-MIE	MO-CONV	DO-MIE	DO-CONV
Dentin-composite interface	Fully bonded	Peak	6.54	4.54	3.82	2.92
		Median	0.37	0.58	0.2	0.31
Enamel-composite interface	Partially debonded	Peak	57.47	285.04	13.02	49.54
		Median	2.59	4.75	0.67	2.36

3.3. Stress distributions of fully-debonded teeth

With the resin composite fully debonded from both enamel and dentin, more extensive stress concentrations could be seen in the CONV models than in the fully-bonded and partially debonded models (Fig. 2). In contrast, the MIE models did not show such changes under the different bonding conditions. There was a discontinuity in the stress distribution across the enamel-composite interface due to complete debonding of the resin composite in the CONV models. A tensile stress concentration of ~8 MPa extended mesial-distally along the central groove to the opposite marginal ridge of the CONV models. The buccal surface of the MO-CONV cavity and the lingual surface of the DO-CONV cavity also contained tensile stress concentrations of ~6 MPa.

Within the coronal and root dentin, there was a further increase in the peak and median values of MPS in all the models (Table 2, Fig. 5). More extensive stress concentration area could be seen on the lateral walls of the pulp chamber and the gingival walls of the cavities compared with the fully-bonded and partially-debonded models (Fig. 3). The CONV models had a higher MPS in the coronal dentin than the MIE models. The DO-MIE model exhibited the lowest peak and median MPS in both the coronal and root dentin.

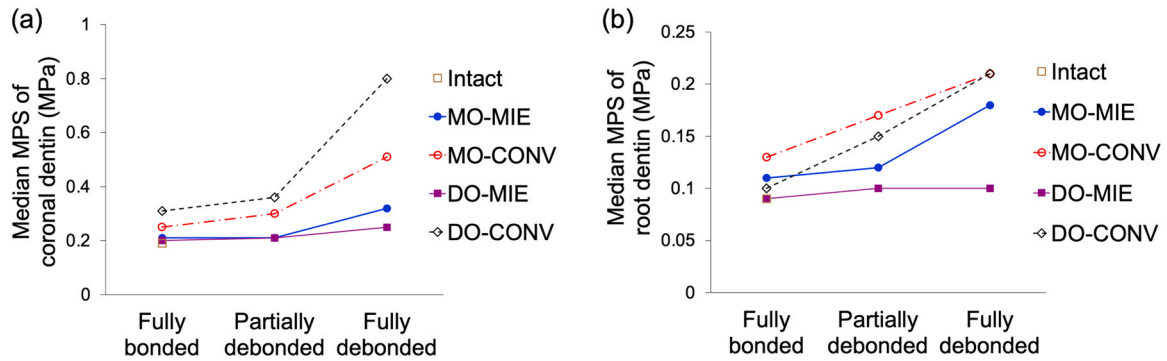| Table 4 – Risk factors of all groups under different bonding conditions.						
		Intact	MO-MIE	MO-CONV	DO-MIE	DO-CONV
Fully bonded	Dentin	0.02	0.02	0.02	0.02	0.02
	Dentin-composite interface	–	0.62	0.43	0.36	0.28
Partially debonded	Dentin	–	0.06	0.35	0.03	0.05
	Enamel-composite interface	–	3.7	20.00	0.83	3.23
Fully debonded	Dentin	–	0.18	0.15	0.03	0.10

Fig. 5 – Median values of MPS (MPa) of coronal dentin (a) and root dentin (b) with different cavity designs and bonding conditions.
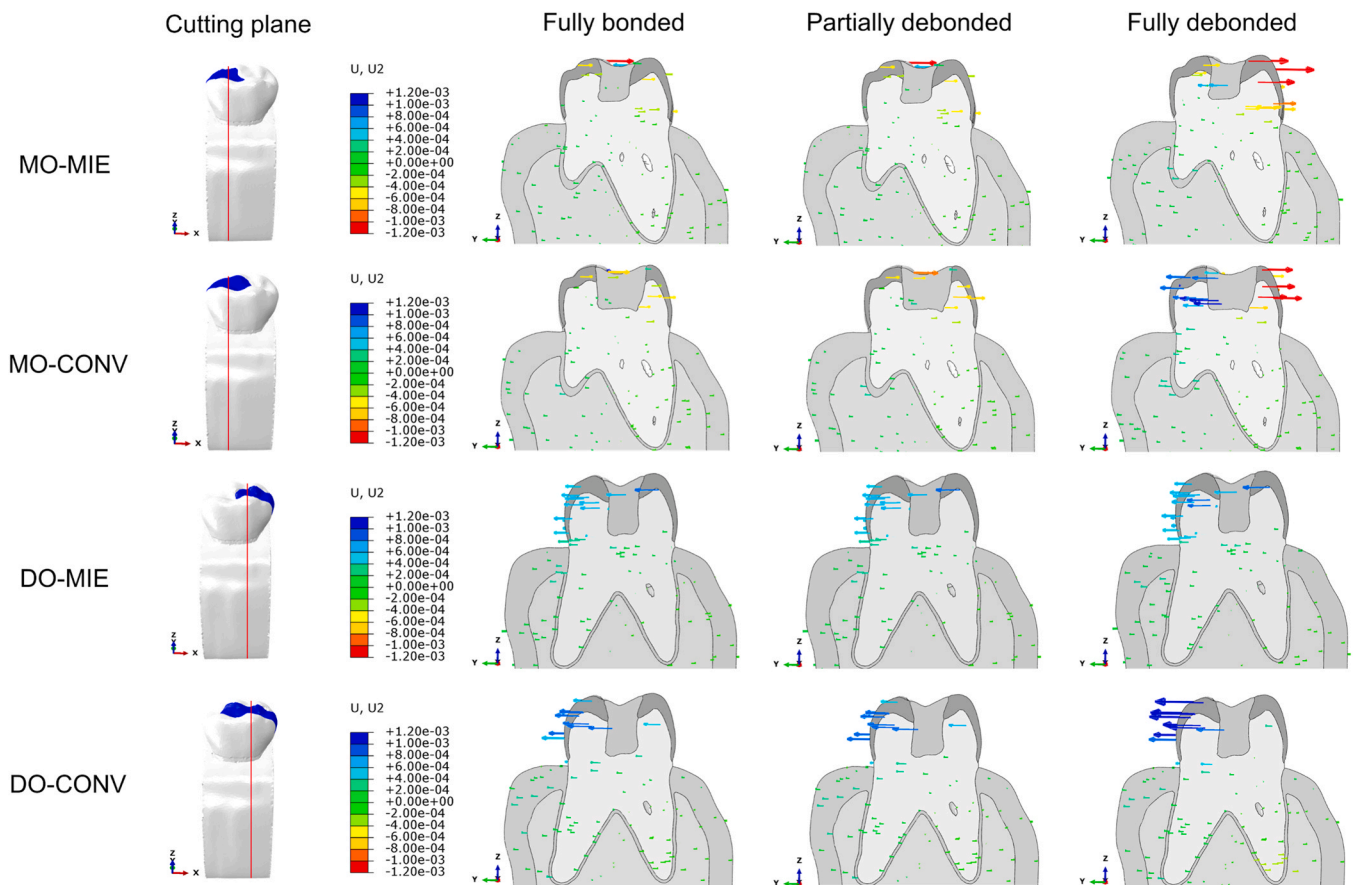

Fig. 6 – Cuspal flexure (mm) of different models under different bonding conditions in the buccopalatal direction from sectional views.

The cuspal flexure in the buccopalatal direction of each model increased significantly compared with that of the fully-bonded or partially-debonded models, explaining the significant increase of tensile stresses in dentin through bending of the cusps after debonding (Fig. 6).

The risk factors of the MO models were higher than those of the DO models (Table 4). The DO-MIE model had the lowest risk factor, which indicated that it would be the last one to fracture following debonding.

4.   Discussion

Cracks and fractures may occur in restored teeth with endodontic treatments [36,37]. Many FEA studies have attempted to understand the fracture of these teeth by focusing on the stress concentrations in dentin [18–23]. However, few studies have considered the role of debonding of the dentin-composite interface or enamel-composite interface, something that is not uncommon to see clinically [14,15], in the

fracture process. In some cases, debonding occurs at the pulpal floor or gingival wall of the interproximal cavity, making it difficult to detect [13]. Regardless, debonding of the restoration would alter the stress distribution within the tooth. Thus, it is important to investigate its influence on the occurrence of cracks and cuspal flexure in endodontically-treated teeth. To address this problem, this study used FEA to analyze different access cavity preparation designs considering different interfacial bonding conditions. This non-destructive method can reveal the most vulnerable regions and highlight other contributing factors [38].

The risk of dentin fracture was evaluated using the peak and median values of the MPS while the risk of interfacial debonding was evaluated using the interfacial normal tensile stresses. Dentin is a brittle material that is weaker under tensile stresses than under compressive stresses. Thus, the MPS is the most significant parameter in evaluating the possible fracture of dentin [39]. For interfaces, the interfacial tensile stress is considered the leading cause for debonding [39]. Thus, these stresses were used in this study to calculate the respective risk factors, defined as the ratio between the failure-causing stress and the material strength, to evaluate the likelihood of failure of the components when comparing the different designs of access cavities [30,31].

It was shown in our study that the different access cavity designs and bonding conditions produced significantly different stresses and risk factors for dentin and the interfaces.

In the fully-bonded teeth, the dentin-composite interface had a higher failure probability than dentin. This indicated that, under normal mastication function, debonding of the dentin-composite interface would happen before the development of dentinal cracks. The likelihood of debonding could be increased by several factors in a proximally-restored tooth, such as the contamination of the gingival wall due to blood and saliva, inadequate curing due to the attenuation of curing light at the deep end of the cavity, polymerization shrinkage of the resin composite, among others [13,16,17]. It appeared that, though the resin composite could be bonded to dentin using a dental adhesive, their interface is still the weakest link of the whole structure [40].

It was shown in our study that the MPS of dentin increased substantially after debonding at the dentin-composite interface or enamel-composite interface, and the risk factor of dentin increased accordingly. Cuspal flexure in the buccopalatal direction also increased significantly after complete debonding of the resin composite, explaining the significant increase in failure-causing tensile stresses of dentin. The bonding status of the resin composite was rarely considered in most studies on the mechanical behavior of restored teeth. Thus, the stresses in dentin might have been underestimated so far. This point should be borne in mind when studying the load capacity of restored teeth in the future.

In the fully-debonded teeth, the CONV models showed higher median stresses and larger stress concentration areas in dentin than the MIE models. This indicated that minimally invasive access cavities could better safeguard the fracture resistance of an interproximally-restored tooth. This could be due to the preservation of a larger volume of tooth structure, especially tooth-strengthening structures such as the pericervical dentin [26,41]. The stress distributions of the CONV models were significantly altered by interfacial debonding, extending mesial-distally along the central groove to the opposite marginal ridge of the cavity. This stress path was very similar to that of crack propagation in cracked restored teeth seen clinically [42]. Thus, it could be speculated that the mesial-distal cracks found in cracked restored teeth were a consequence of stresses caused by debonding of the resin composite. In contrast, the MIE models did not show much difference in their stress distributions before and after debonding. This indicated that minimally invasive access cavities could minimize the adverse effects on the load capacity of a restored teeth induced by interfacial debonding.

5. Conclusion

Within the limitation of this study, it was shown that debonding of resin composite restorations could increase the stresses in dentin and hence the risk of dentin fracture in restored teeth. Minimally invasive access cavities could better safeguard the fracture resistance of interproximally-restored teeth compared to more extensive conventional access cavities.

Conflict of interest

The authors declare that there is no conflict of interest.

Acknowledgment

REFERENCES

[1] Ricucci D, Siqueira JF. Bacteriologic status of non-cavitated proximal enamel caries lesions. A histologic and histobacteriologic study. J Dent 2020;100:103422.

[2] Ausiello P, Ciaramella S, Garcia-Godoy F, Gloria A, Lanzotti A, Maietta S, et al. The effects of cavity-margin-angles and bolus stiffness on the mechanical behavior of indirect resin composite class II restorations. Dent Mater 2017;33:e39–47.

[3] Ausiello P, Ciaramella S, Martorelli M, Lanzotti A, Gloria A, Watts DC. CAD-FE modeling and analysis of class II restorations incorporating resin-composite, glass ionomer and glass ceramic materials. Dent Mater 2017;33:1456–65.

[4] Zelic K, Vukicevic A, Jovicic G, Aleksandrovic S, Filipovic N, Djuric M. Mechanical weakening of devitalized teeth: three-dimensional finite element analysis and prediction of tooth fracture. Int Endod J 2015;48:850–63.

[5] Reeh ES, Messer HH, Douglas WH. Reduction in tooth stiffness as a result of endodontic and restorative procedures. J Endod 1989;15:512–6.

[6] Clark D, Khademi J. Modern molar endodontic access and directed dentin conservation. Dent Clin North Am 2010;54:249–73.

[7] Tang W, Wu Y, Smales RJ. Identifying and reducing risks for potential fractures in endodontically treated teeth. J Endod 2010;36:609–17.

[8] Patel S, Rhodes J. A practical guide to endodontic access cavity preparation in molar teeth. Br Dent J 2007;203:133–40.

[9] Schroeder KP, Walton RE, Rivera EM. Straight line access and coronal flaring: effect on canal length. J Endod 2002;28:474–6.

[10] Tüfenkçi P, Yılmaz K. The effects of different endodontic access cavity design and using XP-endo finisher on the reduction of Enterococcus faecalis in the root canal system. J Endod 2020;46:419–24.

[11] Molina B, Glickman G, Vandrangi P, Khakpour M. Evaluation of root canal debridement of human molars using the GentleWave System. J Endod 2015;41:1701–5.

[12] Neelakantan P, Khan K, Hei Ng GP, Yip CY, Zhang CF, Pan Cheung GS. Does the orifice-directed dentin conservation access design debride pulp chamber and mesial root canal systems of mandibular molars similar to a traditional access design? J Endod 2018;44:274–9.

[13] Novaes JB, Talma E, Las Casas EB, Aregawi W, Kolstad LW, Mantell S, et al. Can pulpal floor debonding be detected from occlusal surface displacement in composite restorations? Dent Mater 2018;34:161–9.

[14] Angeletaki F, Gkogkos A, Papazoglou E, Kloukos D. Direct versus indirect inlay/onlay composite restorations in posterior teeth. A systematic review and meta-analysis. J Dent 2016;53:12–21.

[15] Borgia E, Baron R, Borgia JL. Quality and survival of direct light-activated composite resin restorations in posterior teeth: a 5- to 20-year retrospective longitudinal study. J Prosthodont 2019;28:e195–203.

[16] Aregawi WA, Fok ASL. Shrinkage stress and cuspal deflection in MOD restorations: analytical solutions and design guidelines. Dent Mater 2021;37:783–95.

[17] Rocca GT, Gregor L, Sandoval MJ, Krejci I, Dietschi D. In vitro evaluation of marginal and internal adaptation after occlusal stressing of indirect class II composite restorations with different resinous bases and interface treatments. "Post-fatigue adaptation of indirect composite restorations. Clin Oral Investig. 2012;16:1385–93.

[18] Barbosa AFA, Silva EJNL, Coelho BP, Ferreira CMA, Lima CO, Sassone LM. The influence of endodontic access cavity design on the efficacy of canal instrumentation, microbial reduction, root canal filling and fracture resistance in mandibular molars. Int Endod J 2020;53:1666–79.

[19] Balkaya H, Topçuoğlu HS, Demirbuga S. The effect of different cavity designs and temporary filling materials on the fracture resistance of upper premolars. J Endod 2019;45:628–33.

[20] Sabeti M, Kazem M, Dianat O, Bahrololumi N, Beglou A, Rahimipour K, et al. Impact of access cavity design and root canal taper on fracture resistance of endodontically treated teeth: an ex vivo investigation. J Endod 2018;44:1402–6.

[21] Özyürek T, Ülker Ö, Demiryürek EÖ, Yılmaz F. The effects of endodontic access cavity preparation design on the fracture strength of endodontically treated teeth: traditional versus conservative preparation. J Endod 2018;44:800–5.

[22] Rover G, Belladonna FG, Bortoluzzi EA, De-Deus G, Silva EJNL, Teixeira CS. Influence of access cavity design on root canal detection, instrumentation efficacy, and fracture resistance assessed in maxillary molars. J Endod 2017;43:1657–62.

[23] Plotino G, Grande NM, Isufi A, Ioppolo P, Pedullà E, Bedini R, et al. Fracture strength of endodontically treated teeth with different access cavity designs. J Endod 2017;43:995–1000.

[24] Trivedi S. Finite element analysis: a boon to dentistry. J Oral Biol Craniofacial Res 2014;4:200–3.

[25] Jiang Q, Huang Y, Tu XR, Li Z, He Y, Yang X. Biomechanical properties of first maxillary molars with different endodontic cavities: a finite element analysis. J Endod 2018;44:1283–8.

[26] Yuan K, Niu C, Xie Q, Jiang W, Gao L, Huang Z, et al. Comparative evaluation of the impact of minimally invasive preparation vs. conventional straight-line preparation on tooth biomechanics: a finite element analysis. Eur J Oral Sci 2016;124:591–6.

[27] Chai H. Dentin horn angle and enamel thickness interactively control tooth resilience and bite force. Acta Biomater 2018;75:279–86.

[28] Martin L. Significance of enamel thickness in hominoid evolution. Nature 1985;314:260–3.

[29] Fernandes CP, Glantz POJ, Svensson SA, Bergmark A. A novel sensor for bite force determinations. Dent Mater 2003;19:118–26.

[30] Biewener AA. Safety factors in bone strength. Calcif Tissue Int 1993;53:S68–74.

[31] Baro-Tijerina M, Piña-Monárrez MR, Villa-Covarrubias B. Stress-strength weibull analysis with different shape parameter β and probabilistic safety factor. DYNA 2020;87:28–33.

[32] Zhang Z, Beitzel D, Mutluay M, Tay FR, Pashley DH, Arola D. On the durability of resin-dentin bonds: Identifying the weakest links. Dent Mater 2015;31:1109–18.

[33] Mutluay MM, Yahyazadehfar M, Ryou H, Majd H, Do D, Arola D. Fatigue of the resin-dentin interface: a new approach for evaluating the durability of dentin bonds. Dent Mater 2013;29:437–49.

[34] Vinagre A, Ramos J, Messias A, Marques F, Caramelo F, Mata A. Microtensile bond strength and micromorphology of bur-cut enamel using five adhesive systems. J Adhes Dent 2015;17:107–16.

[35] Beltrami R, Chiesa M, Scribante A, Allegretti J, Poggio C. Comparison of shear bond strength of universal adhesives on etched and nonetched enamel. J Appl Biomater Funct Mater 2016;14:e78–83.

[36] Seo DG, Yi YA, Shin SJ, Park JW. Analysis of factors associated with cracked teeth. J Endod 2012;38:288–92.

[37] Sim IGB, Lim TS, Krishnaswamy G, Chen NN. Decision making for retention of endodontically treated posterior cracked teeth: a 5-year follow-up study. J Endod 2016;42:225–9.

[38] Saberi EA, Pirhaji A, Zabetiyan F. Effects of endodontic access cavity design and thermocycling on fracture strength of endodontically treated teeth. Clin Cosmet Investig Dent 2020;12:149–56.

[39] Huang SH, Lin LS, Fok ASL, Lin CP. Diametral compression test with composite disk for dentin bond strength measurement - Finite element analysis. Dent Mater 2012;28:1098–104.

[40] Purk JH, Dusevich V, Glaros A, Spencer P, Eick JD. In vivo versus in vitro microtensile bond strength of axial versus gingival cavity preparation walls in Class II resin-based composite restorations. J Am Dent Assoc 2004;135:185–93.

[41] Krishan R, Paqué F, Ossareh A, Kishen A, Dao T, Friedman S. Impacts of conservative endodontic cavity on root canal instrumentation efficacy and resistance to fracture assessed in incisors, premolars, and molars. J Endod 2014;40:1160–6.

[42] Rivera EM, Walton RE. Longitudinal tooth fractures: findings that contribute to complex endodontic diagnoses. Endod Top 2007;16:82–111.

[43] Rho JY, Hobatho MC, Ashman RB. Relations of mechanical properties to density and CT numbers in human bone. Medical Engineering and Physics 1995;17(5):347–55.